Medicinal Chemistry Research (2019) 28:1828–1837
https://doi.org/10.1007/s00044-019-02417-2

MEDICINAL CHEMISTRY RESEARCH

ORIGINAL RESEARCH

Zunyimycin C inhibits the proliferation of lung cancer cells by inducing apoptosis through an AKT-related mechanism

Wei Li[1] · Jie Zheng[1] · Wenhong Wang[2] · Zhongming Qian[3] · Yuxin Bao[1,4]

Received: 29 May 2019 / Accepted: 1 August 2019 / Published online: 16 August 2019

Abstract

Objective Zunyimycin C is a novel halogenated type II polyketide derived from the fermentation product of the *Streptomyces* species with notable antibiotic activity. However, it is still unclear whether zunyimycin C could inhibit the activity of cancer cells. In this study, human lung adenocarcinoma cell line A549, the large-cell lung cancer cell line NCI-H460 and the non-small-cell lung cancer cell line NCI-H1299 were employed to determine the in vitro anticancer properties of zunyimycin C and underlying molecular mechanisms.

Materials and methods The cellular viability and proliferative properties of lung cancer cells were investigated using the Cell Counting Kit-8 and colony formation assay, respectively. The mRNA expression of apoptotic genes related to lung cancer was studied using reverse-transcription polymerase chain reaction. The apoptotic ratio was measured through flow cytometry. The protein expression was visualized via western blotting using specific antibodies.

Results Zunyimycin C could inhibit cell proliferation and induce apoptosis in a dose-dependent manner. The expression levels of apoptosis-related proteins (i.e., BAX, cleaved-caspase-3, and cleaved-caspase-9) were increased compared with the control group. However, the levels of Bcl-2 and phosphorylated AKT were decreased by administration by zunyimycin C.

Conclusions Collectively, these results implied that zunyimycin C could inhibit cell proliferation and induce apoptosis via AKT phosphorylation.

Keywords Zunyimycin C · Lung cancer · Cell proliferation inhibition · AKT · Apoptosis

Introduction

Lung cancer is the most common type of cancer worldwide, and the mortality rate associated with this disease ranks first among all malignancies (Torre et al. 2015; Hong et al. 2015; Chen et al. 2016; Byers and Rudin 2015). Currently, the treatment of solid tumors using chemotherapy is often accompanied by the occurrence of toxic side effects. Moreover, the use of numerous anticancer drugs in clinical practice is affected by the development of drug resistance (Trédan et al. 2007), which eventually leads to treatment failure and great suffering to the patients (Robles and Harris 2017). Therefore, there is an urgent need to actively identify effective drugs for the treatment of lung cancer.

Recently, >60% of anticancer drugs used in clinical practice are derived from natural products (Newman et al. 2003). Among those, plant-derived natural products are rich in resources and have various active ingredients (Hadjithomas et al. 2017; Luo et al. 2014; Chen et al. 2017; Zhou et al. 2017). A lot of valuable traditional Chinese medicines (TCMs) were applied as alternative or complementary medicines in the United States and Europe (Wang et al. 2014). Imperatorin isolated from a TCM *Angelica dahurica* and induced apoptosis of the multidrug-resistant liver cancer cells, triggered by the Mcl-1 degradation (Li et al. 2014). Marine biological resources are also extremely rich, and their antitumor activity is almost prominent (Kang et al. 2017; Mei et al. 2017). It had been reported that

✉ Yuxin Bao
baoyuxin8680915@126.com

1 Research Center for Medicine & Biology, Zunyi Medical University, Zunyi 563000 Guizhou, China

2 Guizhou Provincial College-based Key Lab for Tumor Prevention & Treatment with Distinctive Medicines, Zunyi Medical University, Zunyi 563000 Guizhou, China

3 Laboratory of Neuropharmacology, Fudan University School of Pharmacy, 201203 Shanghai, China

4 Center of Analysis & Measurement, Zunyi Medical University, Zunyi 563099 Guizhou, China

renieranycin M isolated from Thai blue sponge was an effective antilung cancer drug (Pinkhien et al. 2016). However, the microbial metabolites are structurally diverse and possess activity against lung cancer (Barka et al. 2016; Wang et al. 2014; Fouillaud et al. 2016), with the microorganism-derived natural products being linked to particular biological activity, lower toxicity, etc. These products demonstrate advantages over synthetic drugs (Wang et al. 2016), with the main active ingredients including polysaccharides, anthracyclines, organic acid esters, anthraquinones, alkaloids, and macrolides, etc.

Aromatic polyketides are known as an important class of natural products with antitumor activity (Liu et al. 2002), such as phoslactomycins (Kawada et al. 2003). These polyketides are mostly isolated from microorganisms (Herman et al. 2017; Son et al. 2017). Zunyimycin C is a novel halogenated type II polyketide derived from the fermentation product of *Streptomyces* species FJS 31-2 (Lü et al. 2017). The type strain was isolated from the soil of Fanjing Mountain Range in Guizhou Province, China (Chinese Common Species Conservation Center Strain number: CGMCC4.7321). And zunyimycin C has highly similar chemical structures with the anthrone natural product BABX (Kodali et al. 2005). Numerous anthrone derivatives exhibit excellent anticancer activity (Li et al. 2018; Lu et al. 2017). Previous research indicated that zunyimycin C showed a good inhibitory effect on the methicillin-resistant *Staphylococcus aureus* and *Enterococci* (Lü et al. 2017). Currently, the anticancer activity of zunyimycin C on lung cancer cells remains unclear. Therefore, this study was conducted to investigate the effects of zunyimycin C on lung cancer cells and determine the underlying mechanism involved in this process.

Materials and methods

Reagents and antibodies

RPMI-1640 medium and DMEM medium were purchased from Hyclone (Logan, UT, USA), while fetal bovine serum (FBS) was purchased from Biological Industries (Beit Haemek LTD, Israel). Real-time reverse-transcription polymerase chain reaction (RT-PCR) kits were purchased from Takara (Beijing, China). AKT and phosphorylated AKT (p-AKT) (Ser473), Bcl-2, BAX, cleaved-caspase-3, cleaved-caspase-9, β-actin, GAPDH (housekeeping protein, widely used as a standardized control) and peroxidase-conjugated antibodies were purchased from Cell Signaling Technology (Danvers, MA, USA). The Trizol reagent and Fluorescein Isothiocyanate (FITC) Annexin V Apoptosis Detection Kit were purchased from Beyotime (Shanghai, China). Zunyimycin C was provided by the Central Laboratory of the First People's Hospital of Zunyi City, China, and the purity of zunyimycin C was >90%, as measured through high-performance liquid chromatography. Zunyimycin C was dissolved in dimethyl sulfoxide (DMSO) (Sigma, Shanghai, China) as mother liquor and diluted by culture medium before use, the final DMSO concentration in cell culture was <0.1%.

Cell culture

The lung adenocarcinoma cell line A549 and the non-small-cell lung cancer (NSCLC) cell line NCI-H1299 were donated by the Department of Oncology of the Affiliated Hospital of Zunyi City, China. The bronchial epithelial cell line 16HBE was provided by the Central Laboratory of the First People's Hospital of Zunyi City, China. The large-cell lung cancer cell line NCI-H460 was purchased from the China Center for Type Culture Collection. The three lung cancer cell lines were cultured in RPMI-1640 medium containing 12% FBS, 100 U/mL penicillin and 100 μg/mL streptomycin (Solarbio, Beijing, China) in 5% CO_2 at 37 °C. The cell line 16HBE was cultured in DMEM medium containing 10% FBS, 100 U/mL penicillin, and 100 μg/mL streptomycin in 5% CO_2 at 37 °C.

Cell viability

Cell viability was measured using the Cell Counting Kit-8 (CCK-8, Yiyuan Biotechnologies, Guangzhou, China) assay. Four types of cells in the logarithmic growth phase were selected, digested, and counted via trypsinization. The cells were prepared into a cell suspension at a density of 0.6×10^4 cells per well and seeded in a 96-well culture plate with 100 μL per well (four replicate wells per group). The cells were cultured for 24 h at 37 °C, 5% CO_2, and saturated humidity. The medium was changed, with different concentrations (5, 10, 20, 40, 80 μM) zunyimycin C treatment for 24, 48, and 72 h. First, the medium was removed and changed, then 10 μL of CCK-8 solution was added to each well and the plate was incubated for an additional 1.5 h (Shi et al. 2018). The microplate reader (Thermo Fisher Scientific Oy, Vantaa, Finland) detects the absorbance at 490 nm (A) and calculates the percent inhibition. The percent inhibition = (control group A value − zunyimycin C concentration A value)/control group A value × 100%.

Colony formation assay

The colony formation assay was performed to evaluate the colony-forming capability of cells (Pan et al. 2016). Initially, A549, H1299, and H460 cells were treated with 20, 40, 60 μM zunyimycin C (control group contains 0.75‰ DMSO, for the maximum concentration 60 μM zunyimycin

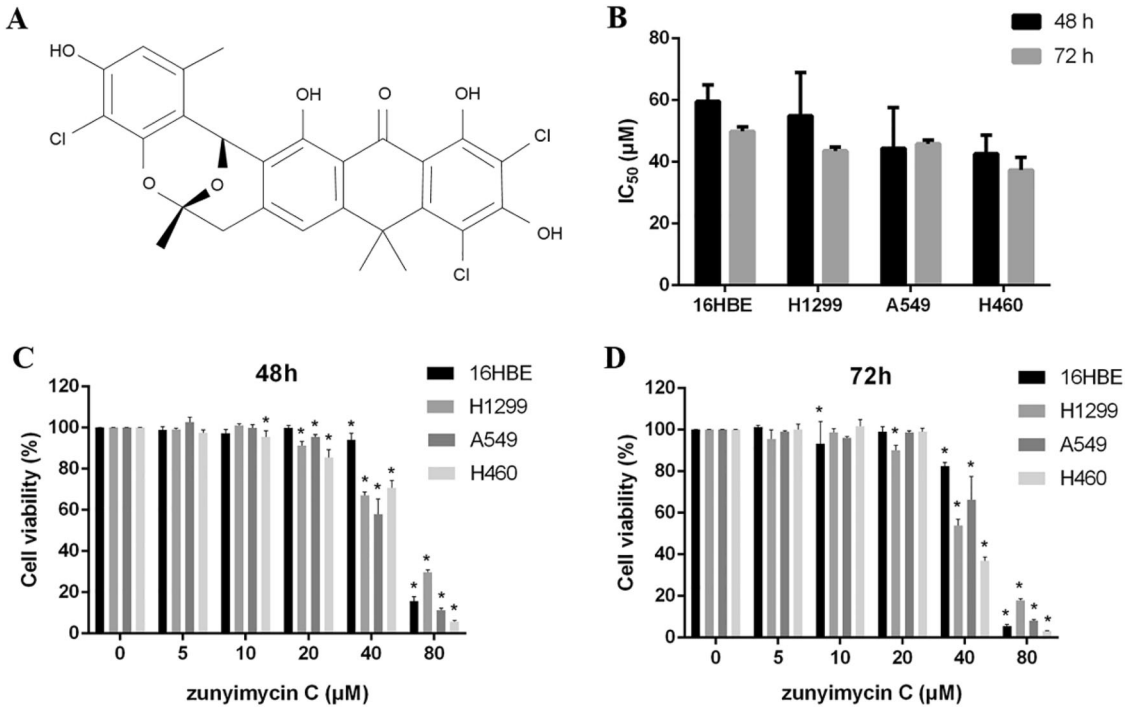

Fig. 1 Zunyimycin C effectively inhibited the proliferation of lung cancer cells. **a** The chemical structure of zunyimycin C. **b** 16HBE, H1299, A549, and H460 cells were treated with the indicated concentrations of zunyimycin C for 48 and 72 h, and IC_{50} values were calculated. **c**, **d** The proliferation of cells was measured using the CCK-8 assay. Data were shown as means ± SD. $*p < 0.05$, compared with the control (0 μM). Data were obtained from at least three independent experiments

C contains 0.75‰ DMSO. The same method was applied in the following assays) for 48 h. Subsequently, the medium was removed, the cells were washed twice with phosphate-buffered saline, collected, and reinoculated in six-well plates at a density of 800 cells per well. The medium was changed every 2 days. After 1 week, the formed colonies were fixed using 10% methanol, followed by staining with 0.1% crystal violet (Solarbio, Beijing, China). The plates were photographed by a digital single lens reflex camera (Canon 5D Mark III, Japan) and the number of colonies was counted.

Annexin V-FITC/propidium iodide (PI) apoptosis assay

Early apoptosis and necrosis were identified via double fluorescence staining with annexin V-PI. Staining for FITC-labeled annexin V binding to membrane phosphatidylserine and PI binding to cellular DNA were detected using an Annexin V-FITC Apoptosis Detection Kit (Beyotime, Shanghai, China) according to the instructions provided by the manufacturer. Briefly, H460, H1299, and A549 cells were seeded in six-well plates at a density of 2×10^5 cells per well. After 24 h, the cells were incubated in the presence or absence of zunyimycin C (20, 40, 60 μM) for 48 h to induce apoptosis. After 48 h treatment, the cells were collected, digested with 0.25% ethylenediaminetetraacetic acid-containing trypsin, and washed twice with phosphate-buffered saline. Approximately 100,000 resuspended cells were centrifuged at 1000 rpm for 5 min, the supernatant was discarded, and the cells were gently resuspended in 195 μL of Annexin V-FITC binding solution. Subsequently, 5 μL of Annexin V-FITC and 10 μL of PI staining solution were added, gently mixed, and incubated at room temperature (20–25 °C) for 10–20 min in the dark. The samples were analyzed using a BD Accuri C6 Plus Flow Cytometer (BD Biosciences, CA, USA).

Western blotting

H460, H1299, and A549 cells were plated in six-well plates at a density of 2×10^5 cells per well. After 24 h, the cells were treated with zunyimycin C at a concentration of 20, 40, and 60 μM. After 48 h, the cells were centrifuged and the pellets were resuspended in cell lysis buffer (50 mM Tris-HCl pH 7.4, 150 mM NaCl, 1 mM ethylenediaminetetraacetic acid, 1% Triton, 0.1% sodium dodecyl sulfate, 5 mg/mL leupeptin, and 1 mM phenylmethane sulfonyl fluoride) for 20 min on ice repeated freezing and thawing for five times. After cold centrifugation at 14,000 rpm for 15 min, the supernatant was collected. The lysed protein was quantified using a Bicinchoninic Acid Protein Assay Kit (Solarbio, Beijing, China). Lysed protein (20 mg) was boiled in 4 × sample buffer and separated through

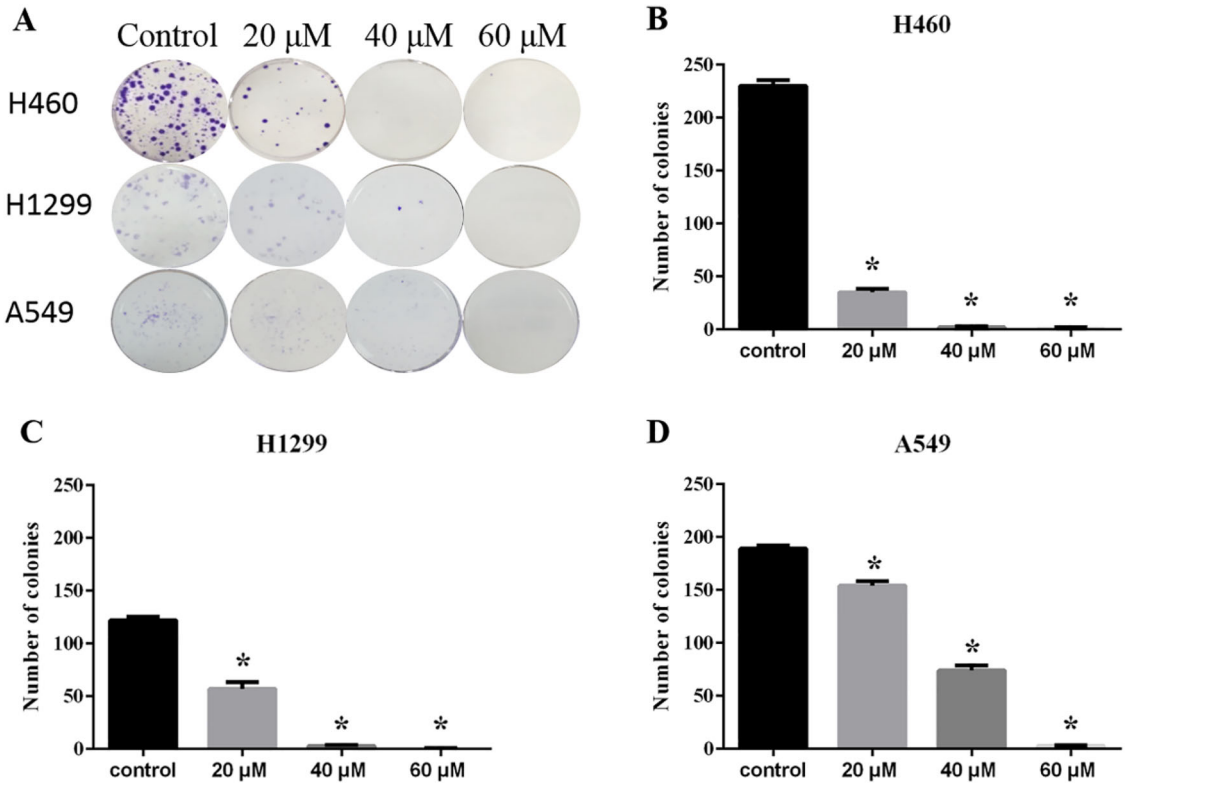

Fig. 2 Zunyimycin C inhibited colony formation in lung cancer cells. The H460, H1299, and A549 cells were treated with 20, 40, and 60 μM of zunyimycin C for 48 h, followed by two washes to remove the compound. Subsequently, the cells were plated to perform the clonogenic assay. **a** Representative images of colonies formed from the three lung cancer cells under different treatment conditions. **b–d** Number of colonies after 7 days, data were shown as means ± SD. *$p < 0.05$, compared with the control. Data were obtained from at least three independent experiments

denaturing sodium dodecyl sulfate polyacrylamide gel electrophoresis (8–12%). Subsequently, the gels were transferred onto a polyvinylidene fluoride membrane and blocked using blocking solution (Beyotime, Shanghai, China) for 1.5 h, followed by overnight incubation at 4 °C with the following primary antibodies: Bcl-2, Bax, cleaved-caspase-3, cleaved-caspase-9, AKT, p-AKT, GAPDH, and β-actin (all 1:1000 dilution). Following incubation with peroxidase-conjugated goat anti-rabbit immunoglobulin G (1:5000 dilution) at room temperature for 2 h, proteins were visualized using the Immobilon Western Chemiluminescent HRP Substrate (Millipore, MA, USA) and detected using the BIO-RAD ChemiDoc Imaging System (Hercules, CA, USA)

Quantitative RT-PCR analysis

Total RNA was extracted using the Trizol reagent (Beyotime, Shanghai, China). Total RNA was used to synthesize the first strand cDNA through the PrimeScript^{TM} RT Master Mix (Perfect Real Time) (Takara, Beijing, China). Real-time PCR amplification was performed using the BioRad CFX 96 Real-Time PCR Detection System (Hercules, CA, USA) according to the instructions provided by the manufacturer for relative quantification. The amplification reaction was performed using the 1 × Power TB Green Premix Ex Taq II (Tli RNaseH Plus) (2×) (Takara, Beijing, China). PCR primers for Bcl-2 (forward, 5′-GGTGGGGTCATGTGTGTGG-3′; reverse, 5′-CGGTTCAGGTACTCAGTCATCC-3′), BAX (forward, 5′-TTTTGCTTCAGGGTTTCATC-3′ reverse, 5′-GACACTCGCTCAGCTTCTTG-3′), and GAPDH (forward, 5′-ACCCAGAAGACTGTGGATGG-3′; reverse, 5′-TTCTAGACGGCAGGTCAGGT-3′) were designed and synthesized by Sangon Biotech (Shanghai, China). The standard temperature profile included initial denaturing at 95 °C for 30 s, followed by 40 cycles of denaturing at 95 °C for 30 s, and annealing and extension at 60 °C for 30 s. A DNA dissociation curve was generated to confirm the specificity of amplification. The relative standard curve method was used to determine the relative mRNA expression using GAPDH as a reference.

Statistical analysis

The SPSS 22.0 software (Chicago, IL, USA) was used to calculate the IC_{50} (concentration for 50% growth inhibition)

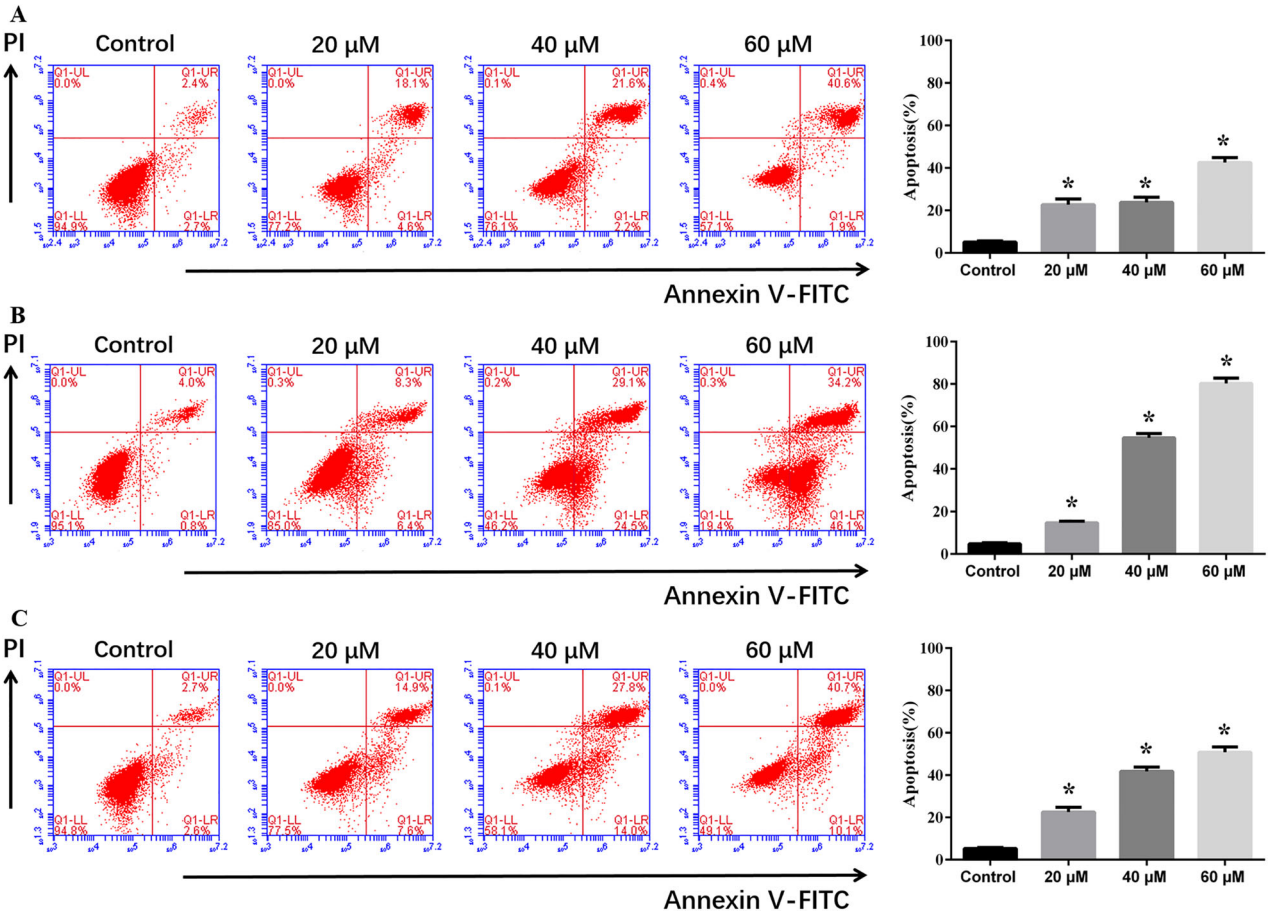

Fig. 3 Zunyimycin C-induced apoptosis in lung cancer cells. The H460, H1299, and A549 cells were treated with 20, 40, and 60 μM of zunyimycin C for 48 h. The rate of apoptosis in these cells was analyzed via flow cytometry. **a**–**c** Representative pictures and quantitative analysis of apoptosis in H460, H1299, and A549 cells. Data were shown as means ± SD. $*p < 0.05$, compared with the control. Data were obtained from three independent experiments

values. Results of the experimental studies were expressed as mean ± standard deviation (SD). All other data analyses were performed using the GraphPad Prism 6 software (La Jolla, CA, USA). One-way analysis of variance was used to compare and analyze the differences between the mean values of multiple groups. A $p < 0.05$ or $p < 0.001$ denoted statistical significance.

Results

Zunyimycin C inhibited the proliferation of lung cancer cells

The 16HBE, H1299, A549, and H460 cell lines were treated with different concentrations (5, 10, 20, 40, and 80 μM) of zunyimycin C and at different times (24, 48, and 72 h). The proliferation of these four types of cells was tested using the CCK-8 assay. The normal 16HBE cells were used as control. After 24 h of culture, the results showed that the growth of cells was not markedly inhibited. However, cell viability was significantly decreased after 48 (Fig. 1c) and 72 h (Fig. 1d). The IC_{50} values were as follows: 59.56 ± 5.42 μM (48 h) and 49.91 ± 1.44 μM (72 h) were the values of 16HBE cells; 54.98 ± 13.97 μM (48 h) and 43.56 ± 1.24 μM (72 h) were the values of H1299 cells; 44.46 ± 13.08 μM (48 h) and 45.85 ± 1.27 μM (72 h) were the values of A549 cells; 42.63 ± 6.00 μM (48 h) and 37.37 ± 4.08 μM (72 h) were for H460 cells (Fig. 1b). As shown in Fig. 1c, d, treatment with zunyimycin C at a concentration <20 μM did not exert a significant inhibitory effect on the four cell lines. In contrast, higher concentrations of the drug (IC_{50} > i.e., >20 μM) induced strong cytotoxicity in the three examined lung cancer cell lines. Notably, toxicity in the normal 16HBE cell line was relatively low. Meanwhile, the assay ultimately determined the adequate concentrations and timings for zunyimycin C test in the next step experiments, which were required to inhibit the proliferation of lung cancer cells without direct cell damage.

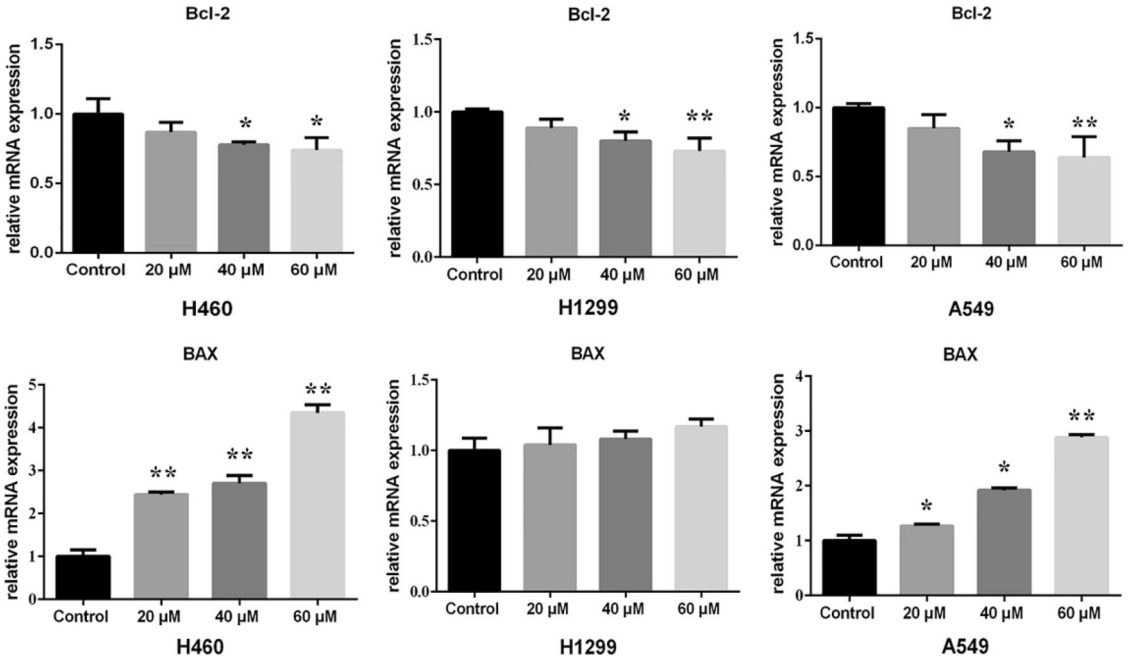

Fig. 4 Relative mRNA expression of target genes in lung cancer cells treated with zunyimycin C (20, 40, 60 μM) for 48 h. Values were presented as the means ± SD with three replicates. *$p < 0.05$ and **$p < 0.001$, compared with the control

Zunyimycin C reduced the colony-forming capability of lung cancer cells

To further demonstrate the antiproliferative activity of zunyimycin C against the H460, H1299, and A549 cells, the effects of the compound on colony formation were measured. As shown in Fig. 2a–d, treatment with zunyimycin C reduced colony formation of lung cancer cells in a dose-dependent manner.

Zunyimycin C-induced apoptosis in lung cancer cells

We hypothesized that zunyimycin C inhibited the proliferation of lung cancer cells was associated with induction of apoptosis. The H460, H1299, and A549 cells were treated with zunyimycin C (20, 40, and 60 μM) for 48 h and stained with PI and Annexin V-FITC antibody to analyze the extent of apoptosis using flow cytometry. As shown in Fig. 3a–c, treatment of lung cancer cells with zunyimycin C (20, 40, and 60 μM) for 48 h induced apoptosis in a dose-dependent manner.

Zunyimycin C regulated the mRNA expression of apoptosis-related genes in lung cancer cells

In order to identify that treatment with zunyimycin C (20, 40, and 60 μM) for 48 h could regulate the mRNA expression of apoptosis-related genes in lung cancer cells. RT-PCR was used to determine the effects of zunyimycin C on the mRNA levels of these genes. As shown in Fig. 4a–c, the expression of *Bcl-2* gene was downregulated, whereas that of *BAX* gene was upregulated compared with the control. In general, the regulation of these genes through treatment with zunyimycin C was dose-dependent.

Zunyimycin C regulated the expression of apoptosis-related proteins in lung cancer cells

To further investigate the underling mechanism of zunyimycin C-induced apoptosis in lung cancer cells. The levels of apoptosis-related proteins (i.e., Bcl-2, BAX, cleaved-caspase-9, and cleaved-caspase-3) were analyzed by western blot. As shown in Fig. 5, after treatment with zunyimycin C (20, 40, and 60 μM) for 48 h, the expression of apoptosis-related proteins (i.e., Bcl-2, BAX) changed. Of note, the expression of Bcl-2 protein was markedly decreased, whereas that of BAX protein was gradually increased (Fig. 5a). Interestingly, treatment with zunyimycin C for 48 h increased the expression of cleaved-caspase-9 and cleaved-caspase-3 proteins in a dose-dependent manner (Fig. 5c). Furthermore, the expression of p-AKT protein was gradually reduced after treatment with zunyimycin C (Fig. 5e). These results indicated that zunyimycin C exerted an antitumor action potentially through regulating the expression level of apoptosis-related proteins in lung cancer cells.

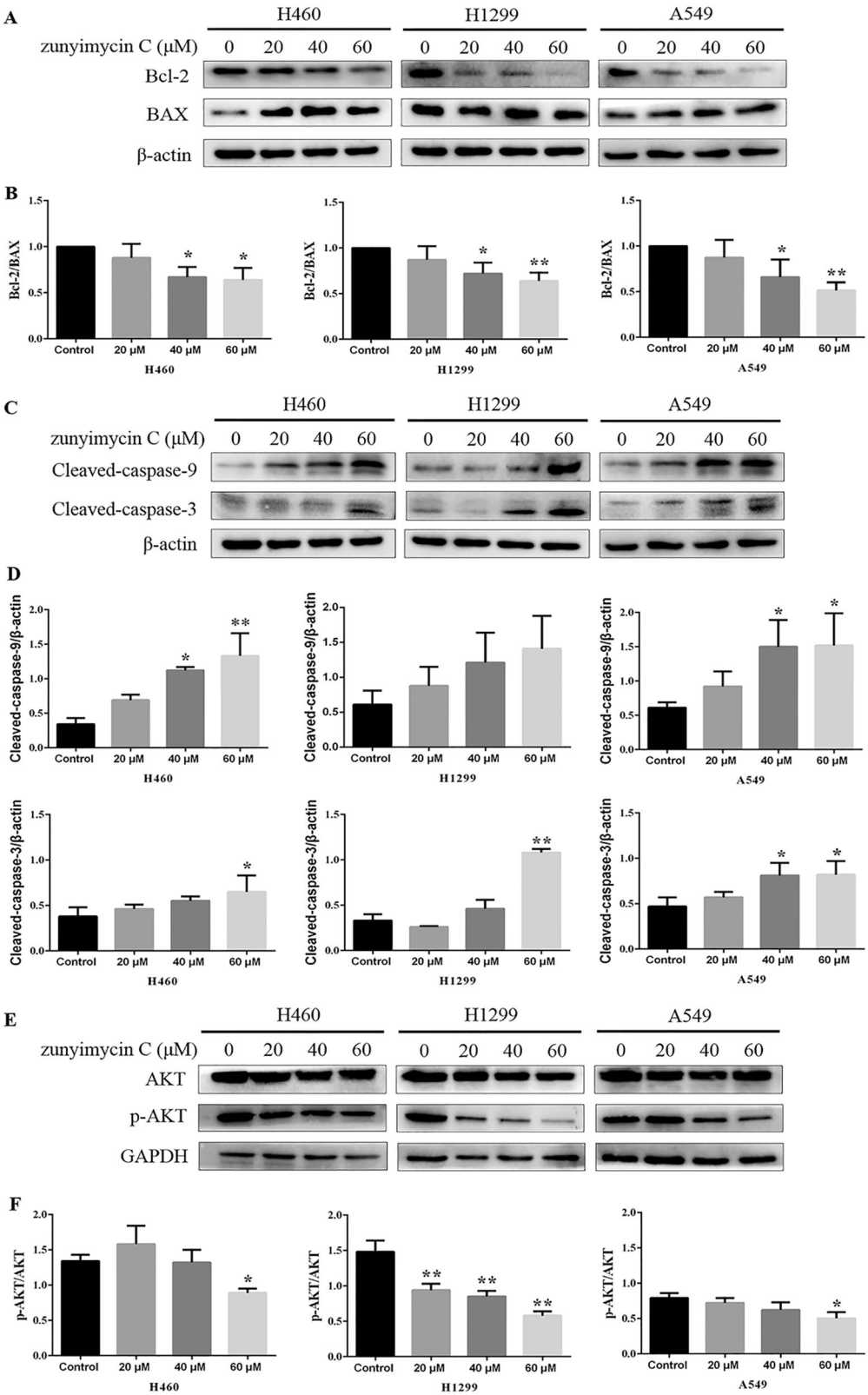

Fig. 5 Zunyimycin C inhibited the expression of phosphorylated AKT and modulated the expression of apoptotic-related proteins in H1299, A549, and H460 cells. Cells were treated with zunyimycin C (20, 40, and 60 μM) for 48 h and the expression of apoptotic-related protein (i.e., Bcl-2, BAX, cleaved-caspase-9, and cleaved-caspase-3) was measured through western blotting. Bar graphs and quantitative analysis for the expression of Bcl-2/BAX (B), cleaved-caspase-3, cleaved-caspase-9 (D), and p-AKT/AKT (F) after treatment for 48 h. β-actin and GAPDH were used as loading controls. Values were presented as the means ± SD. $^{*}p < 0.05$ and $^{**}p < 0.001$ compared with the control. Data were obtained from three independent experiments

Discussion

Natural product resources are abundant, and a large number of small molecular compounds derived from natural product are being used as candidate anticancer agents (Kinghorn et al. 2016; Hua et al. 2017). Zunyimycin C, a secondary metabolite derived from *Streptomyces* species FJS 31-2 with an anthrone-like structure. Numerous studies have shown that anthrone-like compounds are a class of drugs, exhibiting antitumor activity via multi-routes, multi-targets and multi-links (Guise et al. 2014; Wei et al. 2013; Boichuk et al. 2014). In this research, we demonstrated that zunyimycin C inhibited lung cancer cells proliferation and induced apoptosis by modulating the expression of AKT.

Tumor growth involves a complex cascade of events, including progressive cell proliferation and metastasis (Pan et al. 2016). According to the CCK-8 assays, zunyimycin C was cytotoxic against lung cancer cells. Meanwhile, the compound also effectively inhibited colony formation of lung cancer cells in a dose-dependent manner.

Apoptosis is the primary mechanism of programmed cell death in mammalian tissues (Booth et al. 2014). Of note, a decreased rate of apoptosis leads to the development of cancer (Hassan et al. 2014). The permeabilization of the mitochondrial outer membrane is an irreversible point in the process of apoptosis, determined by the complex interactions between the members of the Bcl-2 family (Birkinshaw and Czabotar (2017); Andreu-Fernández et al., (2017)). Tumor cells inhibit apoptosis by upregulating the expression of antiapoptotic proteins (e.g., Bcl-2) or downregulating the expression of proapoptotic proteins (e.g., BAX) (Hassan et al. 2014; Reyna et al. 2017). In this study, we found that zunyimycin C-induced apoptosis in a dose-dependent manner, following a decrease in the expression of Bcl-2 protein and an increase in the expression of BAX protein. And further RT-PCR results also showed that the corresponding expression of Bcl-2 and BAX gene were changed accordingly.

Bcl-2 and BAX were mitochondrial upstream proteins that played as important regulators of mitochondrial membrane permeability and controlled caspase-3 protein activation downstream of mitochondria during apoptosis signaling, among which caspase-3 is an important indicator of apoptosis (Xu et al. 2016; Hansakul et al. 2014). This process would trigger the cleavage activation of caspase-9 and caspase-3, which in turn initiated the caspase cascade to accelerate apoptosis (Zhou et al. 2018; Ahn et al. 2018; Yu et al. 2017). Subsequently, degradation of the DNA damage repair enzyme PARP results in the accumulation of DNA damage in the cells, leading to an increased rate of apoptosis (Deben et al. 2016; Zargoulidis et al. 2015; Fei et al. 2016). Our results showed the upregulation of cleaved-caspase-9 and cleaved-caspase-3 expression in parallel with the increasing concentration of zunyimycin C.

AKT is an important inhibitor of apoptosis proteins in vivo and the core of the PI3K/AKT signaling pathway (Zhu et al. 2016), which is a central node in cell signaling downstream of growth factors, cytokines, and other cellular stimuli (Manning and Cantley 2007). PI3K was known as signaling networks upstream of AKT, when activated by signals from tyrosine kinases and G-protein coupled receptors, it promoted AKT activation, which in turn inhibited cell proliferation and accelerated apoptosis (Franke 2008). Our results showed that zunyimycin C suppressed the phosphorylation of AKT in a concentration-dependent manner. However, the effect of zunyimycin C on the cell cycle of lung cancer cells and the upstream signaling molecules of the PI3K/AKT signaling pathway (e.g., epidermal growth factor receptor, EGFR (Jacobsen et al. 2017)) remain to be investigated. Further, as compared with in vitro, the environment in vivo was extremely complex, the effects of zunyimycin C on the lung cancer cells may not lead to antitumor activity. Therefore, the antitumor activity of zunyimycin C in the lung tumor model needed to be experimentally validated in vivo.

In summary, zunyimycin C exerted antitumor activity on lung cancer cells via inhibition of growth and AKT-mediated induction of apoptosis. Therefore, zunyimycin C may be a promising lead compound in the treatment of lung cancer.

Acknowledgements The Authors would like to thank Yun Liu for his assistance with flow cytometry and Sanhua Li for her technical assistance. Especially, thanks to Changwu Yue for providing test compound of zunyimycin C. This work was funded by the National Nature Science Foundation of China (Grant no. 31460006), the Science and Technology Foundation of Guizhou Province (no. (2013) 3013).

Authors' contributions Study design: YB. Data acquisition: WL. Data analysis and interpretation: YB, ZQ, and WL. Statistical analysis: WL. Manuscript writing: WL. Manuscript editing: YB, ZQ. Manuscript review: WL, JZ, WW, YB, and ZQ.

Compliance with ethical standards

Conflict of interest The authors declare that they have no conflict of interest.

References

Ahn DS, Lee HJ, Hwang J et al. (2018) Lambertianic acid sensitizes non-small cell lung cancers to TRAIL-induced apoptosis via

inhibition of XIAP/NF-κB and activation of caspases and death receptor 4. Int J Mol Sci 19(5):1476
Andreu-Fernández V, Sancho M, Genovés A et al. (2017) Bax transmembrane domain interacts with prosurvival Bcl-2 proteins in biological membranes. Proc Natl Acad Sci USA 114 (2):310–315
Byers LA, Rudin CM (2015) Small cell lung cancer: where do we go from here? Cancer 121:664–672
Barka EA, Vatsa P, Sanchez L et al. (2016) Taxonomy, physiology, and natural products of actinobacteria. Microbiol Mol Biol Rev 80(1):1–43
Boichuk S, Lee DJ, Mehalek KR et al. (2014) Unbiased compound screening identifies unexpected drug sensitivities and novel treatment options for gastrointestinal stromal tumors. Cancer Res 74(4):1200–1213
Booth LA, Tavallai S, Hamed HA et al. (2014) The role of cell signalling in the crosstalk between autophagy and apoptosis. Cell Signal 26(3):549–555
Birkinshaw RW, Czabotar PE (2017) The BCL-2 family of proteins and mitochondrial outer membrane permeabilisation. Semin Cell Dev Biol 72:152–162
Chen W, Zheng R, Baade PD et al. (2016) Cancer statistics in China, 2015. Cancer J Clin 66(2):115–132
Chen Y, Tang Q, Xiao Q et al. (2017) Targeting EP4 downstream c-Jun through ERK1/2-mediated reduction of DNMT1 reveals novel mechanism of solamargine inhibited growth of lung cancer cells. J Cell Mol Med 21:222–233
Deben C, Lardon F, Wouters A et al. (2016) APR-246 (PRIMA-1 (MET)) strongly synergizes with AZD2281 (olaparib) induced PARP inhibition to induce apoptosis in non-small cell lung cancer cell lines. Cancer Lett 375(2):313–322
Fei HR, Tian H, Zhou XL et al. (2016) Inhibition of autophagy enhances effects of PF-04691502 on apoptosis and DNA damage of lung cancer cells. Int J Biochem Cell Biol 78:52–62
Fouillaud M, Venkatachalam M, Girard-Valenciennes E et al. (2016) Anthraquinones and derivatives from marine-derived fungi: structural diversity and selected biological activities. Mar Drugs 14(4):64
Franke TF (2008) PI3K/Akt: getting it right matters. Oncogene 27 (50):6473–6488
Guise CP, Mowday AM, Ashoorzadeh A et al. (2014) Bioreductive prodrugs as cancer therapeutics: targeting tumor hypoxia. Chin J Cancer 33(2):80–86
Hadjithomas M, Chen IA, Chu K et al. (2017) IMG-ABC: new features for bacterial secondary metabolism analysis and targeted biosynthetic gene cluster discovery in thousands of microbial genomes. Nucleic Acids Res 45(D1):D560–D565
Hansakul P, Aree K, Tanuchit S, Itharat A (2014) Growth arrest and apoptosis via caspase activation of dioscoreanone in human non-small-cell lung cancer A549 cells. BMC Complement Altern Med 14:413
Hassan M, Watari H, AbuAlmaaty A et al. (2014) Apoptosis and molecular targeting therapy in cancer. Biomed Res Int 2014:150845
Herman NA, Kim SJ, Li JS et al. (2017) The industrial anaerobe *Clostridium acetobutylicum* uses polyketides to regulate cellular differentiation. Nat Commun 8(1):1514
Hong QY, Wu GM, Qian GS et al. (2015) Prevention and management of lung cancer in China. Cancer 121:3080–3088
Hua F, Shang S, Hu ZW (2017) Seeking new anti-cancer agents from autophagy-regulating natural products. J Asian Nat Prod Res 19 (4):305–313
Jacobsen K, Bertran-Alamillo J, Molina MA et al. (2017) Convergent Akt activation drives acquired EGFR inhibitor resistance in lung cancer. Nat commun 8(1):410
Kang Y, Wang ZJ, Xie D et al. (2017) Characterization and potential antitumor activity of polysaccharide from Gracilariopsis lemaneiformis. Mar Drugs 15(4):100
Kawada M, Kawatsu M, Masuda T et al. (2003) Specific inhibitors of protein phosphatase 2A inhibit tumor metastasis through augmentation of natural killer cells. Int Immunopharmacol 3(2):179–188
Kinghorn AD, DE Blanco EJ, Lucas DM et al. (2016) Discovery of anticancer agents of diverse natural origin. Anticancer Res 36 (11):5623–5637
Kodali S, Galgoci A, Young K et al. (2005) Determination of selectivity and efficacy of fatty acid synthesis inhibitors. J Biol Chem 280(2):1669–1677
Lü Y, Shao M, Wang Y et al. (2017) Zunyimycins B and C, new chloroanthrabenzoxocinones antibiotics against methicillin-resistant *Staphylococcus aureus* and *Enterococci* from *Streptomyces* sp. FJS31-2. Molecules 22(2):251
Liu W, Christenson SD, Standage S, Shen B (2002) Biosynthesis of the enediyne antitumor antibiotic C-1027. Science 297(5584): 1170–1173
Li JS, Zhang H, Qi H et al. (2018) Bioactive naphthoquinone and anthrone derivatives from endophytic Micromonospora sp. NEAU-gq13. J Asian Nat Prod Res 26:1–10
Li X, Zeng X, Sun J et al. (2014) Imperatorin induces Mcl-1 degradation to cooperatively trigger Bax translocation and Bak activation to suppress drug-resistant human hepatoma. Cancer Lett 348(1-2):146–155
Lu C, Zhao Y, Jia WQ et al. (2017) A new anthracycline-type metabolite from *Streptomyces* sp. NEAU-L3. J Antibiot 70(10): 1026–1028
Luo X, Luo W, Lin C et al. (2014) Andrographolide inhibits proliferation of human lung cancer cells and the related mechanisms. Int J Clin Exp Med 7:4220–4225
Manning BD, Cantley LC (2007) AKT/PKB signaling: navigating downstream. Cell 129(3):1261–1274
Mei C, Zhou S, Zhu L et al. (2017) Antitumor effects of laminaria extract fucoxanthin on lung cancer. Mar Drugs 15(2):39
Newman DJ, Cragg GM, Snader KM (2003) Natural products as sources of new drugs over the period 1981–2002. J Nat Prod 66:1022–1037
Pan LL, Wang XL, Zhang QY et al. (2016) Boehmenan, a lignan from the Chinese medicinal plant *Clematis armandii*, induces apoptosis in lung cancer cells through modulation of EGF-dependent pathways. Phytomedicine 23(5):468–476
Pinkhien T, Maiuthed A, Chamni S et al. (2016) Bishydroquinone renieramycin M induces apoptosis of human lung cancer cells through a mitochondria-dependent pathway. Anticancer Res 36 (12):6327–6333
Reyna DE, Garner TP, Lopez A et al. (2017) Direct activation of BAX by BTSA1 overcomes apoptosis resistance in acute myeloid leukemia. Cancer Cell 32(4):490–505
Robles AI, Harris CC (2017) Integration of multiple "OMIC" biomarkers: a precision medicine strategy for lung cancer. Lung Cancer 107:50–58
Shi H, Bi H, Sun X et al. (2018) Antitumor effects of tubeimoside-1 in NCI-H1299 cells are mediated by microRNA-126-5p-induced inactivation of VEGF-A/VEGFR-2/ERK signaling pathway. Mol Med Rep 17(3):4327–4336
Son S, Ko SK, Jang M et al. (2017) Polyketides and anthranilic acid possessing 6-deoxy-α-l-talopyranose from a *Streptomyces* species. J Nat Prod 80(5):1378–1386
Torre LA, Bray F, Siegel RL et al. (2015) Global cancer statistics, 2012. Cancer J Clin 65:87–108
Trédan O, Galmarini CM, Patel K, Tannock IF (2007) Drug resistance and the solid tumor microenvironment. J Natl Cancer Inst 99:1441–1454

Wang CY, Bai XY, Wang CH (2014) Traditional Chinese medicine: a treasured natural resource of anticancer drug research and development. Am J Chin Med 42:543–559

Wang M, Li Y, Shao M et al. (2014) Separation and phylogenetic analysis of actinomycetes with activity of against *Candida albicans* from Chishui danxia soil. J Zunyi Med Univ 37(4):404–408.

Wang Y, Shao M, Yue C (2016) Research development of halogenated natural products derived microorganisms. J Zunyi Med Univ 39(4):435–440.

Wei WT, Lin SZ, Liu DL, Wang ZH (2013) The distinct mechanisms of the antitumor activity of emodin in different types of cancer (Review). Oncol Rep 30(6):2555–2562

Xu P, Cai X, Zhang W et al. (2016) Flavonoids of Rosa roxburghii Tratt exhibit radioprotection and anti-apoptosis properties via the Bcl-2(Ca^{2+})/Caspase-3/PARP-1 pathway. Apoptosis 21(10): 1125–1143

Yu P, Shi L, Song M, Meng Y (2017) Antitumor activity of paederosidic acid in human non-small cell lung cancer cells via inducing mitochondria-mediated apoptosis. Chem Biol Inter 269:33–40

Zarogoulidis P, Petanidis S, Kioseoglou E et al. (2015) MiR-205 and miR-218 expression is associated with carboplatin chemoresistance and regulation of apoptosis via Mcl-1 and Survivin in lung cancer cells. Cell Signal 27(8):1576–1588

Zhou L, Wu F, Jin W et al. (2017) Theabrownin inhibits cell cycle progression and tumor growth of lung carcinoma through c-myc-related mechanism. Front Pharm 8:75

Zhou R, Chen H, Chen J et al. (2018) Extract from Astragalus membranaceus inhibit breast cancer cells proliferation via PI3K/AKT/mTOR signaling pathway. BMC Complement Alter Med 18:83

Zhu X, Jiang H, Li J et al. (2016) Anticancer effects of Paris saponins by apoptosis and PI3K/AKT Pathway in gefitinib-resistant non-small cell lung cancer. Med Sci Monit 22:1435–1441